Structure of $T=2$ ^{24}Ne from ^{14}C on ^{14}C

C. R. Hoffman, S. L. Tabor, M. W. Cooper, T. Baldwin, D. B. Campbell, C. Chandler, K. W. Kemper, J. Pavan, A. Pipidis, M. A. Riley, and M. Wiedeking
Department of Physics, Florida State University, Tallahassee, Florida 32306, USA

B. A. Brown
National Superconducting Cyclotron Laboratory and Department of Physics and Astronomy, Michigan State University, East Lansing, Michigan 48824, USA

(Received 21 May 2003; published 5 September 2003)

The ^{14}C(^{14}C,α) reaction at 22 MeV was used to study $T=2$ ^{24}Ne. Charged particles were detected with a Si detector telescope at 0°, and γ transitions in coincidence were detected with an array of three Compton-suppressed ''clover'' detectors and seven Compton-suppressed single Ge crystals. The α-γ and α-γ-γ coincidence data were analyzed to study the structure of ^{24}Ne. Twenty-two new γ lines were assigned to 14 new levels. Angular distribution measurements provided spin assignments and restrictions to a number of levels. Likely candidates were found for the lowest 5^+ and 6^+ levels. All but one of the 12 states predicted to lie below 6 MeV by shell model calculations using the universal *s-d* interaction were observed. The rms deviation in excitation energies among these is 190 keV, and there is a tendency for the observed levels to lie somewhat higher than the predicted ones. A comparison of the structure of ^{24}Ne with its neighbors suggests a significant shell gap above the $\nu d_{5/2}$ orbital in agreement with the large $d_{5/2}$-$s_{1/2}$ gap implied by the effective single-particle energies in the universal *s-d* shell model interaction.

DOI: 10.1103/PhysRevC.68.034304 PACS number(s): 27.30.+t, 23.20.Lv, 23.20.En, 21.60.Cs

I. INTRODUCTION

Nuclei in the *s-d* shell with low isospin T ($N \approx Z$) have been well studied, both experimentally and theoretically. The region provides an excellent testing ground for structure theory since there are enough particles to provide good examples of collective motion and enable macroscopic calculations, yet few enough to permit wide basis microscopic calculations. Shell model calculations allowing all particles beyond the ^{16}O core to occupy the full *s-d* shell with an interaction fitted to much of the experimentally known structure in the shell, the universal *s-d* (USD) interaction, have been very successful in describing a wide range of nuclear properties in this mass region [1]. For example, USD calculations predicted well the recently observed first 10^+ state in ^{24}Mg [2]. Both microscopic USD and macroscopic cranked Nilsson-Strutinsky model calculations have correctly predicted that the fully aligned $\frac{13}{2}^+$ and $\frac{17}{2}^+$ states in ^{25}Mg lie below the collective rotational states of the same spins [3,4].

In contrast, experimental results thin out rapidly with increasing isospin. Only a few $T=2$ excited states are known in the *s-d* shell, and the first $T=\frac{5}{2}$ γ decay scheme (for ^{27}Na) was presented in 2002 [5]. Such studies are important for testing how the nuclear structure responds to increasing neutron-proton imbalance and how well models account for it. This is particularly true for astrophysical network calculations which rely heavily on shell model calculations for the properties of high T nuclei.

The $T=0$ structure of ^{24}Mg has long been known to be rather collective. Earlier, it was thought that this collectivity should extend to other isospin states of the $A=24$ system, including $T=2$ ^{24}Ne, especially since the lighter even Ne isotopes exhibit rotation-like spectra. Although ^{24}Ne is difficult to reach experimentally, challenging experiments using the ^{22}Ne(t,p) reaction began to reveal a more vibration-like level scheme. This suggested that, with a closed neutron $d_{5/2}$ shell, the structure of ^{24}Ne with two active protons should closely resemble that of ^{18}O with two neutrons in the *s-d* shell. However, shell model calculations with an earlier version of the USD interaction provided good agreement with what was experimentally known then and indicated that the structure is more complicated than any of these simple pictures [6]. Many questions remain about whether a more extensive level scheme of ^{24}Ne would continue to agree with the USD calculations based on the low T structure of *s-d* shell nuclei or might point the way to changes in the model leading to better understanding of more neutron-rich nuclei.

All of the prior works on the excitation spectrum of ^{24}Ne have used the (t,p) reaction, beginning with a pioneering (t,p) measurement [7]. Eight excited states were observed up to 6 MeV. Spins of $2\hbar$ were assigned to the first two excited states at 1981 and 3871 keV in an early ($t,p\gamma$) angular correlation experiment using a NaI scintillator as the γ detector [8]. A (t,p) angular distribution measurement assigned $\ell=2$ (and hence positive parity) to the 3871-keV level and 0^+ to the 4765-keV state [9]. In the same work, a p-γ angular correlation study of the unresolved 1981-keV doublet established 4^+ for the 3962-keV third excited state. Lifetimes were measured for the 1981-keV 2_1^+ and 4765-keV 0_2^+ states and a limit was set for the 3871-keV 2_2^+ level using the Doppler shift attenuation method [10,11]. A more recent (t,p) angular distribution measurement [12] has identified 29 excited states up to 11.47 MeV with spin restrictions on a number of states and an assignment of 0^+ to a state at 5.70 MeV from a distorted-wave Born approximation analysis of the proton angular distributions.

The recent availability of a radioactive, albeit long-lived,

^{14}C beam and a ^{14}C target in conjunction with a modern γ detector array has allowed the possibility of exploring the structure of $T=2$ ^{24}Ne with a heavy-ion reaction for the first time. It offered the possibility to better understand the role of increasing isospin in the $A=24$ system and of more detailed tests of theories for the structure of nuclei with greater neutron excess.

II. EXPERIMENTAL TECHNIQUE

The nucleus ^{24}Ne was populated in the ^{14}C(^{14}C,α) reaction at $E_{\rm lab}=22$ MeV with beam intensities averaging 3×10^{10} particles/s from the Florida State University Superconducting Accelerator Laboratory. The ^{14}C beam was produced in a dedicated Cs sputter ion source with an enriched Fe_3C sample [13]. A self-supporting ^{14}C foil 600 μg/cm^2 thick was used as the target. Charged particles from the reaction were detected and identified with a 5-mm-thick E detector and a 150-μm ΔE detector placed at 0° relative to the beam and subtending 0.82 sr of solid angle. A 27-mg/cm^2 Au foil placed between the target and particle detectors was used to stop the ^{14}C beam. The FSU array of Compton-suppressed Ge detectors was used to detect coincident γ rays. Three four-crystal clover detectors and one single-crystal detector were placed at 90° relative to the beam. Two single-crystal detectors were placed at 35° and four more at 145°. Add-back mode was used for the clover detectors except for the angular distribution analysis. Signals in the E detector in coincidence with any γ detector provided the trigger for data acquisition.

A. Particle-γ coincidences

The ^{14}C(^{14}C,2n)^{26}Mg reaction accounted for about 98% of the total reaction cross section. Lines from ^{24}Ne could only be seen in coincidence with α particles, which were well separated from the other light charged particles in the E-ΔE plane. A portion of the γ spectrum in coincidence with α particles is shown in Fig. 1 as an example. The ^{22}Ne lines result from a small ^{12}C contamination on the target. This contamination has been observed in other reaction channels as well [5], but does not pose a problem because the level scheme of ^{22}Ne is well known and the reaction on ^{12}C has a different Q value.

The α-γ correlations provide valuable information about the placement of new energy levels and γ transitions. One way of examining these correlations is illustrated in Fig. 2. Two regions of the γ spectrum are shown in coincidence with four different ranges of α particle energies. The highest α energy range (shown on top) corresponds to the excitation energy region of the first 2^+ state at 1981 keV. Only the 1981-keV transition is visible in this spectrum. The next α gate corresponds to the 4-MeV-excitation-energy region and includes decays from the second 2^+ state (1890 keV) and the first 4^+ state (1981 keV), as well as subsequent $2_1^+\rightarrow0^+$ decays (1981 keV). More ^{24}Ne γ lines appear in the lower energy α gates, corresponding to higher regions of excitation energy.

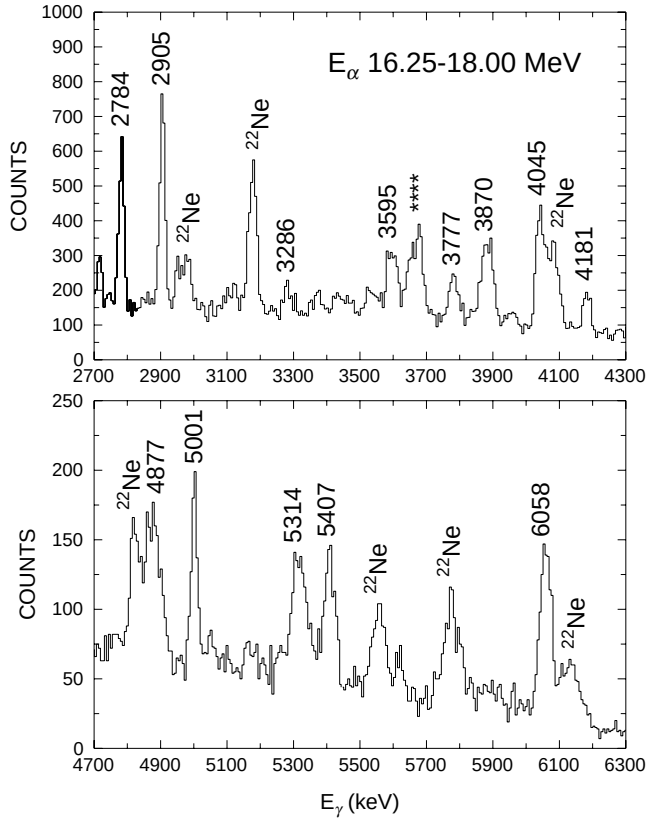

FIG. 1. Portions of the γ spectrum in coincidence with a limited range of α energies. Transitions in ^{24}Ne are labeled by their energies in keV, while those labeled by "^{22}Ne" result from the ^{12}C contamination on the target. The peak labeled by "****" is an unresolved combination of several lines from 3654 to 3677 keV. This spectrum and all the other γ spectra in this paper have been corrected for Doppler shifting.

Note that because decays from higher lying states tend to cascade through lower energy levels, decays from these lower energy levels appear in coincidence with a wide range of α particle energies. For example, the 1981-keV doublet grows in relative intensity with lower α energies (higher excitation energies). Thus, when examining the α-γ correlations by gating on γ lines, the highest coincident α energies correspond to direct population of the state emitting the γ ray. This is illustrated in Fig. 3 which shows the α spectra in coincidence with a number of different γ lines. The α particles in coincidence with the 1981-keV line from the lowest excited state in ^{24}Ne extend to the highest energy. Therefore, the highest coincident α energies indicate the placement of each γ decay line.

The kinematic relation between α energy and excitation energy is shown by nearly straight lines in Fig. 4 for the (^{14}C,α) reactions on both ^{14}C and the contaminant ^{12}C. The data points are plotted at the measured maximum α energies E_α and the excitation energies E_x inferred from the level scheme and decay energies. The excitation energies of the ^{22}Ne levels and the lower ^{24}Ne levels were previously known. For new ^{24}Ne levels, this graph provides placement information and a consistency check.

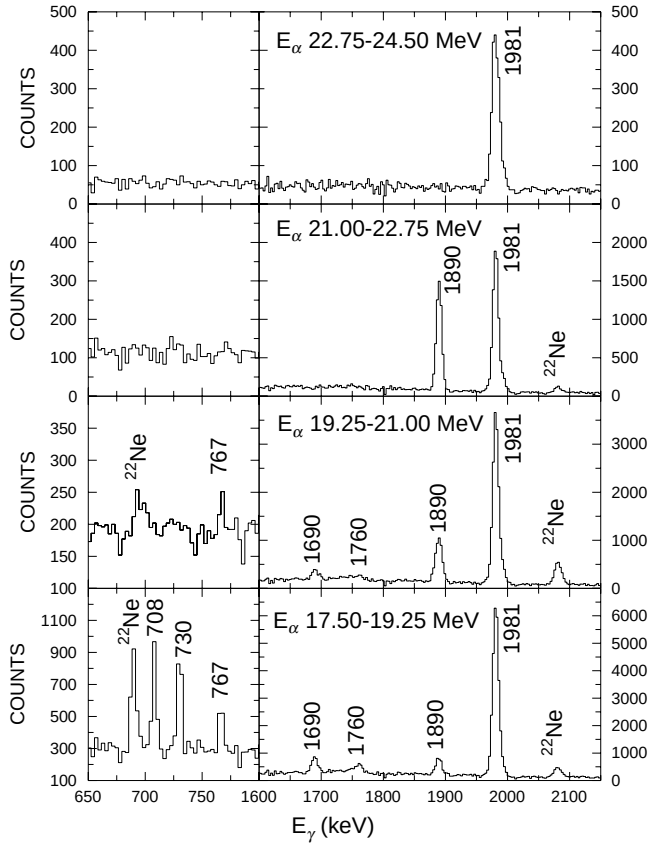

FIG. 2. Portions of the γ spectra in coincidence with four adjacent ranges of α energy corresponding to four regions of excitation energy in ^{24}Ne. The peaks are labeled as in Fig. 1.

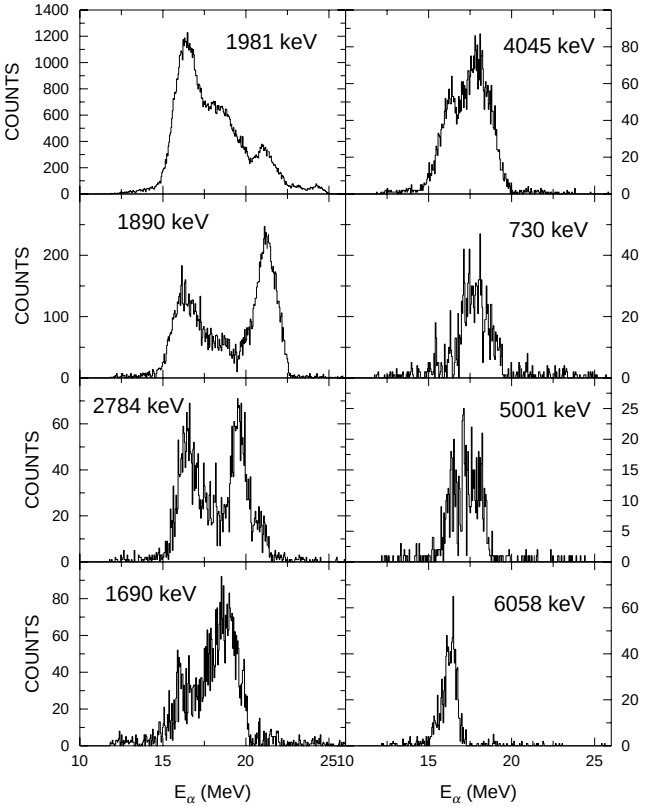

FIG. 3. α spectra in coincidence with the indicated γ lines.

Although particle-γ coincidences provided the experiment trigger, a moderate number of α-γ-γ coincidences were also recorded. These provided additional evidence for placement of the γ lines in the level scheme. Some examples of the α-γ-γ coincidences are shown in Figs. 5 and 6. The previously known coincidence of the 1981-keV line with itself can clearly be seen in Fig. 5.

B. Angular distributions

It was possible to obtain two-point angular distributions for many of the γ decays. While a minimum of three points is needed to determine both a_2 and a_4 coefficients of the Legendre polynomials of order 2 and 4 expected for dipole-quadrupole radiation, the two-point angular distributions still provide useful information for assigning spins. Since $\cos^2(35°)=\cos^2(145°)$, the γ detectors at 35° and 145° were combined to produce one spectrum in a special sorting for measuring angular distributions. The effects of different angular distributions can be seen in Fig. 7 where the same regions of the γ spectra at $35°+145°$ and 90° in coincidence with α particles of any energy are compared. The 708-keV line is weaker and the 730- and 767-keV lines are stronger at 90°.

The four individual Ge crystals in each clover detector are about the same size as the single-crystal detectors, so the efficiency of all the detectors should have a similar variation with energy. A special sorting was made of just the 90° detectors in which multiple hits in a clover detector were vetoed, rather than added together. Although this led to the loss of some counts, the veto mode avoided treating the clover

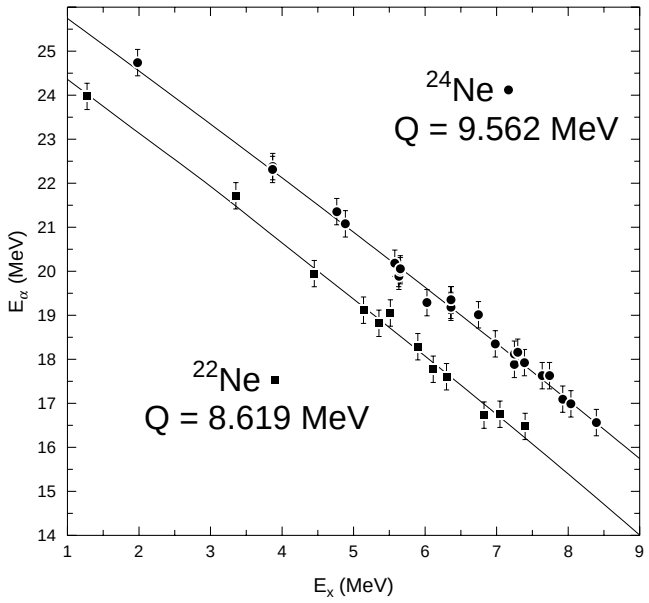

FIG. 4. Highest α energy in coincidence with a given γ line vs the excitation energy of the state from which the γ decay occurs. The expected correlations from kinematics calculations are shown as lines.

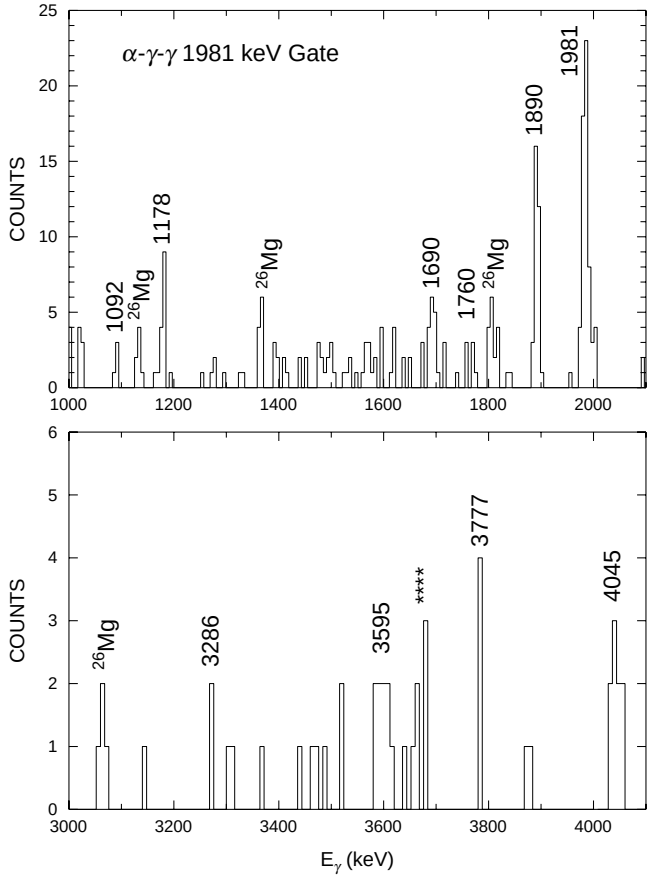

FIG. 5. Portions of the γ spectrum in coincidence with α particles and 1981-keV γ rays in another detector. The peak labeled by "****" is an unresolved combination of several lines from 3654 to 3677 keV.

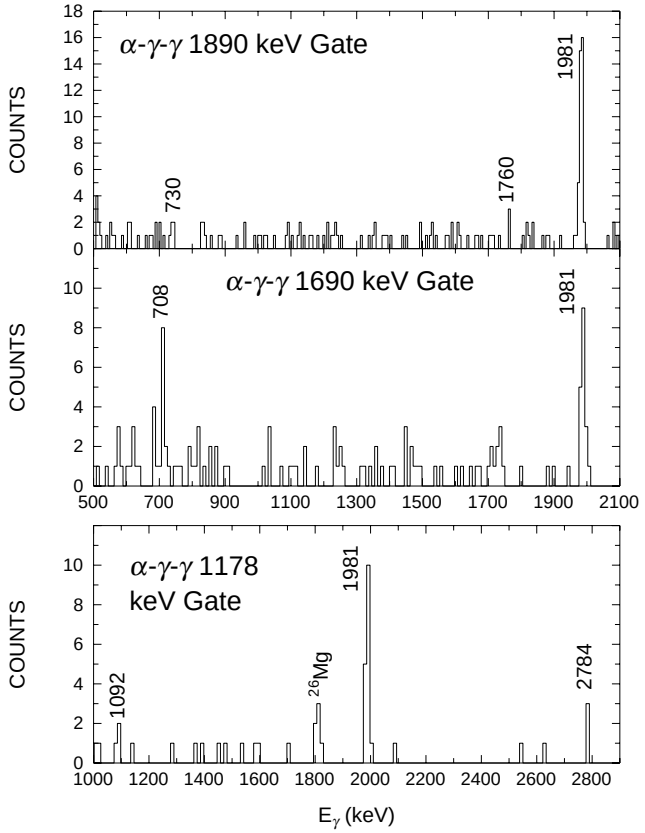

FIG. 6. Portions of the γ spectra in coincidence with α particles and the indicated γ lines.

detectors (all positioned at 90°) as larger Ge crystals whose efficiency would not decrease as rapidly with energy as would that of the individual crystals. Thus the relative normalization of the 90° versus $35°+145°$ detectors should be independent of energy. This normalization was determined from the 2784-keV γ line depopulating the 0_2^+ state at 4765 keV whose angular distribution must be isotropic. The normalization was found to be consistent with that determined from the decays of some $\frac{1}{2}^+$ states in ^{25,27}Na (from the t and p coincidences) whose angular distributions must also be isotropic in the absence of polarization.

The angular distributions were fitted assuming a Gaussian distribution of magnetic substate populations with a width of $\sigma=1.6\hbar$. This value of σ was determined by fitting angular distributions of known transitions in ^{22}Ne arising from the ^{12}C contaminant on the target.

III. RESULTS

The construction of the level scheme for ^{24}Ne, shown in Fig. 8, will be discussed in this section. The comparison with USD shell model calculations, shown on the left side of Fig. 8, will be discussed in the following section.

Although it was not possible to measure lifetimes in the present work, there is no evidence for reduced Doppler shifting on any peaks, which implies that all lifetimes must be less than about 1 ps and the observed decays must proceed by $E1$, $M1$, and/or $E2$ radiation.

A spin of $2\hbar$ was assigned to the first excited state in ^{24}Ne at 1981 keV from a $(t,p\gamma)$ angular correlation experiment [8]. Positive parity was established by the measurement of a mean lifetime of 0.89 ps [10], which implies a reasonable $E2$ strength of 7.2 W.u., but an unreasonably large $M2$ strength. Our angular distribution measurement of 1.30(8) for the ratio of yield at $35°+145°$ to that at 90° is quite consistent with this assignment.

A spin of $2\hbar$ was also assigned to the second excited state at 3871 keV from the $(t,p\gamma)$ angular correlation [8]. An $\ell=2$ assignment in a (t,p) angular distribution experiment [9] implies positive parity. As shown in the top left panel of Fig. 9, the present γ angular distribution for the 1890-keV line provides an excellent fit to that expected for a $2\rightarrow2$ decay with a mixing ratio of $\delta=-0.18$, which is quite consistent with the value of $\delta=-0.15(15)$ reported in Ref. [8].

$J=4$ was assigned to the third excited state at 3962 keV from a simultaneous analysis of the unresolved $4\rightarrow2$ and $2\rightarrow0$ decay angular correlations [9]. The doublet nature of the 1981-keV γ line is demonstrated in Fig. 5, where a 1981-keV line clearly appears in the 1981-keV gate. While the $2\rightarrow0$ decay can be isolated by an α energy gate, as shown in the top panel of Fig. 2, it is very difficult to isolate the $4\rightarrow2$ decay. However, no differences have been observed in the centroids of the 1981-keV line in different gates, so it is

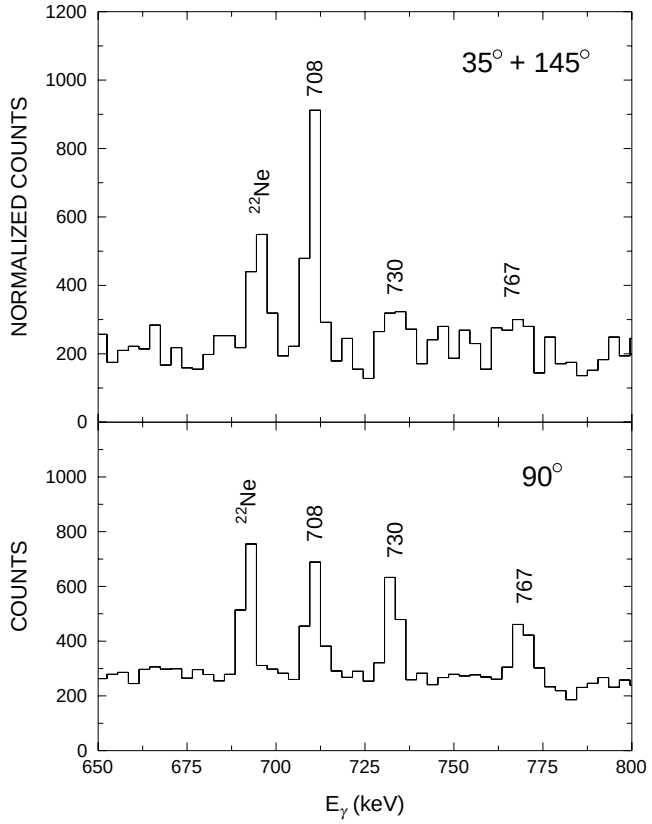

FIG. 7. Comparison of a portion of the γ spectrum at 35° $+145°$ with that at 90° in coincidence with α particles.

likely that the two lines differ by less than 1 keV in energy.

An $\ell=0$ (t,p) angular distribution [9] established 0^+ for the fourth excited state at 4765 keV. Little was previously known about the fifth excited state at 4886 keV except for its presence as a shoulder on the peak for the 4765-keV state in (t,p) spectra and an observation of its dominant decay to the 2_1^+ level. This decay mode (2905 keV) has been seen in the present work, and no other decay branches could be observed. Fits to its angular distribution are shown in the top right panel of Fig. 9 for possible spins of $1\hbar$ through $4\hbar$. A spin hypothesis of $0\hbar$ (not shown since only $\delta=0$ is possible) gives a poor fit with $\chi^2\sim10$. The fit for $1\hbar$ is poor for all δ values, as is that for $4\hbar$ at $\delta=0$, which is the only physically reasonable value. This leaves spins of 2 and $3\hbar$. The nonzero mixing ratio for $3\hbar$ and lifetime limits mentioned earlier rule out a mixed $E1/M2$ decay mode and thus rule out 3^-. The angular distribution of the 767-keV line feeding into this state rules out $2\hbar$, leaving an assignment of 3^+ for the 4886-keV state.

A spin of $2\hbar$ was assigned to the 5576 keV level in Ref. [9], and the measured angular distribution of its 3595-keV decay line is consistent with 2^+. The nonzero mixing ratio rules out 2^-. A weak (t,p) peak at 5.641(25) MeV was tentatively recognized in an early experiment [7], while a peak at 5.70(6) MeV was unambiguously assigned $\ell=0$ in the latest work [12]. With the higher resolution of the Ge detector array, we have observed two states in this region at 5631 and 5653 keV. The 5653 keV state cannot be the 0^+ level seen in (t,p) because of its decay to the 4^+ state. Also the angular distribution of the 1760-keV decay of the 5631-

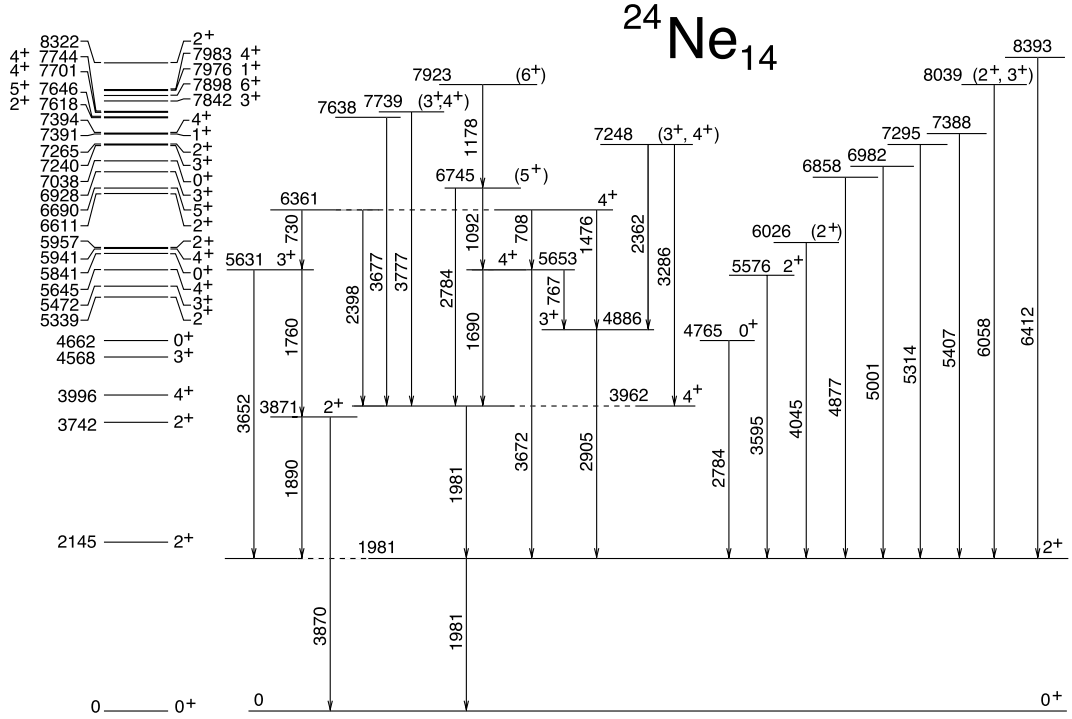

FIG. 8. Level and decay scheme of ^{24}Ne based on the present and previous work. Shell model predictions using the USD interaction are shown on the left.

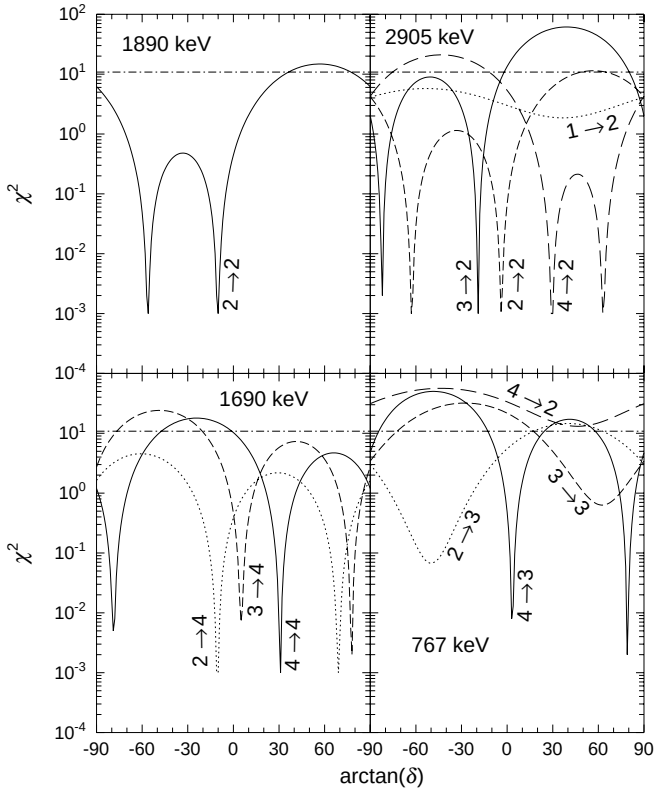

FIG. 9. Graphs of the goodness of fit χ^2 of theoretical calculations for the indicated γ lines with the indicated spin hypotheses to the measured angular distributions as a function of the arctangent of the mixing ratio δ. The 0.1% confidence limit is shown as a dot-dashed horizontal line near the top of each graph.

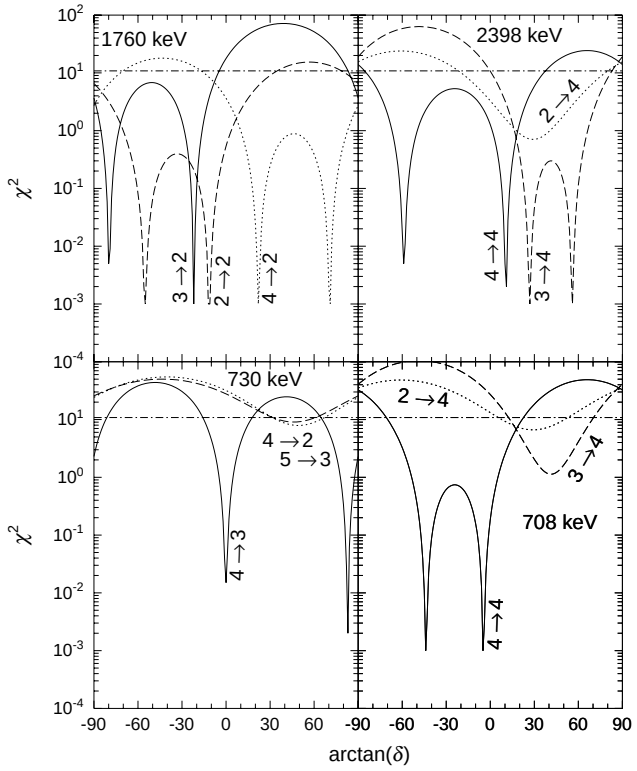

FIG. 10. Same as Fig. 9 for other γ lines.

keV state [ratio=1.21(8)] is not consistent with the isotropic one a spin 0 state must have. Thus it appears that the third 0^+ state was not populated strongly enough in the present reaction to be visible.

The 5631-keV state decays nearly equally to the first and second 2^+ levels. Fits to the angular distribution of the 1760-keV decay are shown in Fig. 10. A spin hypothesis of $4\hbar$ gives a poor fit at the only physically reasonable δ value of 0. Spins of 2 and $3\hbar$ both give good fits at reasonably small mixing ratios. The nonzero values of these mixing ratios imply positive parity since $M2$ decay would not be consistent with the lifetime limits mentioned earlier. The angular distribution of the 730-keV transition feeding into this state rules out spin 2, leaving an assignment of 3^+ for the 5631-keV level.

Fits to the 767- and 1690-keV decays of the 5653-keV state are shown in Fig. 9. Both spins of 3 and 4 give good fits to the angular distribution of the 1690-keV line, while the fit for spin 2 at zero mixing ratio is marginal. Only spin 4 gives a good fit for the 767-keV angular distribution for the small values of δ expected for this relatively low energy transition in which $E2$ decay should be weak. Thus the 5653-keV level has spin-parity 4^+, since the nonzero mixing ratio for the 1690-keV decay would imply an unreasonably large $M2$ strength.

The 6026-keV state probably corresponds to the one observed at 6.030(18) MeV [7] or 6.07(6) MeV [12], and a spin-parity of (2^+) was suggested in the latter study. The angular distribution of the 4045-keV decay line is consistent with 2^+ with a nonzero mixing ratio which rules out 2^-. The 6361-keV state likely corresponds to the (t,p) peak at 6.37(6) MeV in Ref. [12]. Possible spin-parities of 2^+ or 3^- were suggested for this state [12], but the limited features in the (t,p) angular distribution make an assignment difficult and the 4^+ curve fits about as well. Angular distribution fits for the 708-, 730-, and 2398-keV decays of the 6361-keV state are shown in Fig. 10. Clearly, only spin 4 gives good fits for all the lines and the nonzero mixing ratio for the 2398-keV line implies positive parity. Also, the 730-keV angular distribution rules out $2\hbar$ for the 5631-keV level, as mentioned earlier.

Above this, the level density increases, and it becomes more difficult to determine the correspondence between states observed in the present work and those seen in the (t,p) reaction [12]. An exception is the likely correspondence between the strong (t,p) peak at the 8.04(6)-MeV (whose angular distribution implies 2^+ or 3^+) and the 8039-keV state. The α-γ-γ coincidences provide additional evidence for the placement of some of the higher lying states. Some examples are the 3286-, 3595-, 3654-, 3677-, 3777-, and 4045-keV lines in Fig. 5. The 1092-, 1981-, and 2784-keV lines in the 1178-keV α-γ-γ gate shown in Fig. 6, in addition to α cutoff energies, provide the placement of the 6745- and 7923-keV levels. Note that the 2784-keV lines represent the second doublet in this nucleus, after the 1981-keV lines. The decays of these two states by relatively low energy transitions (1092 and 1178 keV) suggest higher spins,

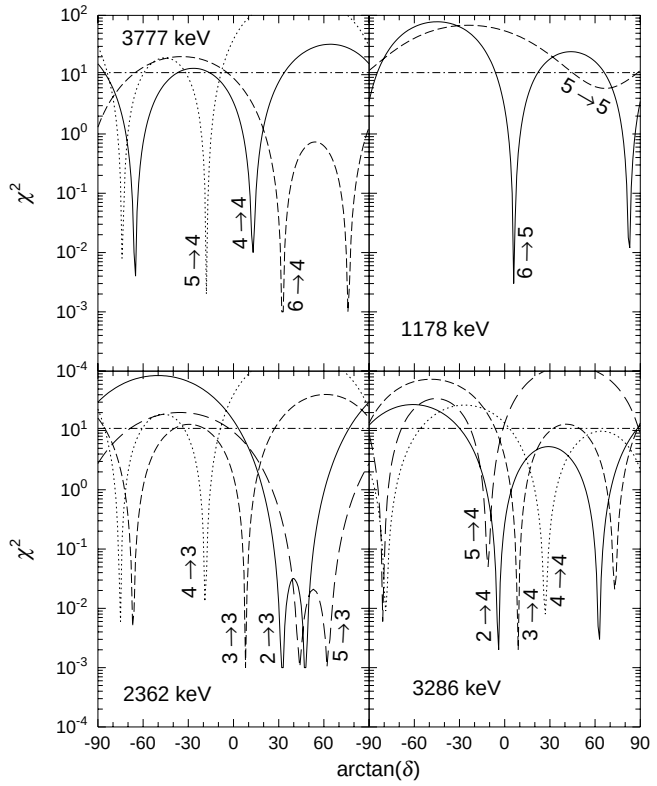

FIG. 11. Same as Fig. 9 for other γ lines.

since many other higher energy decays would be open to lower spin states. It was not possible to extract a reliable angular distribution for the 1092-keV line, but that of the 1178-keV transition, shown in Fig. 11, implies a pure dipole decay. Likely spins for the 6745- and 7923-keV states will be discussed in the following section.

Fits to the angular distributions of the 2362- and 3286-keV decays of the 7248-keV state are also shown in Fig. 11. Together they are consistent with spin-parity values of 2^+, 3^+, 3^-, or 4^+. The 7638- and 7739-keV states are also candidates for higher spins, since they decay exclusively (as far as we can tell) to the lowest 4^+ state. The fits to the angular distribution of the 3777-keV decay of the 7739-keV level, shown in Fig. 11, are consistent with 3^+, 4^+, or 5^+, but not with 6^+, which must have $\delta=0$. It was not possible to measure the angular distribution of the 3677-keV decay of the 7638-keV state because of other nearby lines.

The observed γ decays and the lifetime limits provide restrictions on the possible spins, even when reliable angular distributions could not be obtained. For example, the decays of the 6858-, 6982-, 7388-, 8039-, and 8393-keV states to the lowest 2^+ level limit their possible spin-parities to 0^+, 1, 2, 3, or 4^+.

IV. DISCUSSION

A. USD shell model

As mentioned earlier, shell model calculations allowing all particles outside the ^{16}O core to occupy the full s-d shell and using an effective interaction fitted to the structure of many s-d shell nuclei (USD) have been very successful in describing the positive-parity states in nuclei across the shell [1]. For $T=2$ ^{24}Ne, the previously known states at 1981, 3871, 3962, and 4765 keV were included in the (USD) fit.

There is a rather clear correspondence of states below 5 MeV with the shell model predictions (Fig. 8), although most of these (along with many from other nuclei) were included in the fit to the interaction. The root-mean-square (rms) deviation between the five predicted and observed states is 142 keV, which is quite typical of the agreement seen in other s-d shell nuclei.

Another observable which can be compared to model predictions is the decay pattern. Observed and predicted decay branching ratios are compared in Table I. There is good agreement in the decay patterns up to 5 MeV excitation energy, although this is partly constrained by the limited number of levels to which the states can decay. The largest difference is for the decay of the 5631-keV 3^+ state. The small branching ratio to the 1981-keV 2^+ level is determined in the theory by a very small $B(M1)$ value of $0.000\,39\mu_N^2$, whereas the $B(M1)$ strength for the $3_1^+\rightarrow 2_1^+$ transition is $0.029\mu_N^2$. A very small remixing of the two 3^+ states would raise the $B(M1)$ value for the $3_2^+\rightarrow 2_1^+$ transition to $0.004\mu_N^2$ and account for the nearly 50% decay branch observed.

If the 0^+ state observed in the (t,p) reaction [12] at 5.70(6) MeV, but not seen in the present work, is included, then six states are observed and predicted by the USD calculations between 5 and 6.5 MeV. The spin assignments discussed in the preceding section lead to a one to one correspondence with the shell model states (as shown in Table I) and an rms deviation of 230 keV, which is somewhat higher than that of the states below 5 MeV (and none of these states was included in the fit to the interaction). The correspondence between predicted and observed decay patterns is good for the 5576-, 5653-, and 6026-keV states, but poor for the 5631- and 6361-keV ones. The reason for the poor agreement is not clear. Even if one ignores the spin assignments, it is not possible to rearrange the correspondence between experimental and theoretical states to significantly improve the agreement in decay patterns.

In the region of 6.5–8 MeV, nine states have been observed in the present work, while 16 are predicted in the shell model calculations and additional intruder states are also possible. Thus, a full identification between predicted and observed states is not possible. Some likely correspondences can be pointed out, however.

The 6745- and 7923-keV states are excellent candidates for the predicted lowest 5^+ and 6^+ states at 6690 and 7898 keV. Their energies and decay patterns agree well with shell model predictions. (Because of the 2784-keV doublet, only approximate decay branching ratios for the 6745-keV state can be determined from the 1178-keV gate.) Furthermore, no state in the region other than the 6^+ one is predicted to decay predominately to a level only about an MeV below it.

Identification of the 7248-keV state is much less clear. The predicted 3^+ state at 7240 keV would be a perfect match in energy, but no measurable decay branches are predicted for either of the observed decays to the lowest 3^+ and 4^+

TABLE I. Comparison between the observed decay branching ratios (BR) of states in ^{24}Ne and those predicted by the *s-d* shell model using the USD interaction. The last column shows the difference between the observed and predicted excitation energies.

		Experiment			Shell model		
E_i (keV)	J_i^π	J_f^π	E_f (keV)	BR (%)	E_x (keV)	BR (%)	ΔE (keV)
1981	2^+	0^+	0	100	2145	100	-164
3871	2^+	0^+	0	8	3742	6	129
		2^+	1981	92		94	
3962	4^+	2^+	1981	100	3996	100	-34
4765	0^+	2^+	1981	100	4662	100	103
		2^+	3871	<3		0	
4886	3^+	2^+	1981	100	4568	96	318
		2^+	3871	<3		4	
5576	2^+	0^+	0	<2	5339	1	237
		2^+	1981	100		95	
		2^+	3871	<4		4	
5631	3^+	2^+	1981	49	5472	4	159
		2^+	3871	51		92	
		4^+	3962	<3		4	
5653	4^+	2^+	1981	34	5645	23	8
		2^+	3871	<1		1	
		4^+	3962	58		56	
		3^+	4886	8		20	
5700[a]	0^+				5841		(-141)
6026	2^+	2^+	1981	100	5957	93	69
		3^+	4886	<5		4	
		3^+	5631	<2		3	
6361	4^+	2^+	1981	<4	5941	26	420
		2^+	3871	<4		3	
		4^+	3962	23		65	
		3^+	4886	<14		3	
		3^+	5631	30		3	
		4^+	5653	47		<1	
6745	(5^+)	4^+	3962	65	6690	63	58
		3^+	4886	<5		6	
		4^+	5653	35		27	
		4^+	6361	<5		4	
7923	(6^+)	4^+	3962	<18	7898	30	27
		4^+	5653	<3		7	
		(5^+)	6745	100		63	

[a]Reference [12].

levels. The 4^+ state at 7394 keV is not far away with a predicted 96% decay branch to the first 4^+ level. This is perhaps the best match among the shell model states, but no measurable branch is predicted to the 3_1^+ level. Another quite viable possibility is that the 7248-keV level is an intruder 3^- state.

The 7739-keV experimental state is another possible candidate to correspond to the predicted 4^+ state at 7394 keV. Compared to the 7248-keV candidate, the energy is farther away, but the decay only to the 4_1^+ level matches perfectly. The predicted 5_2^+ state at 7646 keV is a better match in energy for the 7739-keV experimental level with a predicted 34% decay branch to the 4_1^+ state. However, no evidence has been seen for the predicted 60% decay branch to the 4_3^+ level. The 7739-keV state is less likely to have negative parity because the mixing ratio of its decay γ line is not consistent with zero for any of the spin possibilities. The experimental 7638-keV state is also a candidate for the same shell model states. Again the predicted 7394-keV level is the only nearby one whose decay pattern agrees and there are two other experimental candidates for this level.

B. Intruder states

The question remains of negative-parity intruder states involving a particle or hole in an orbital below or above the *s-d* shell. The possibility of such states introduces a wild

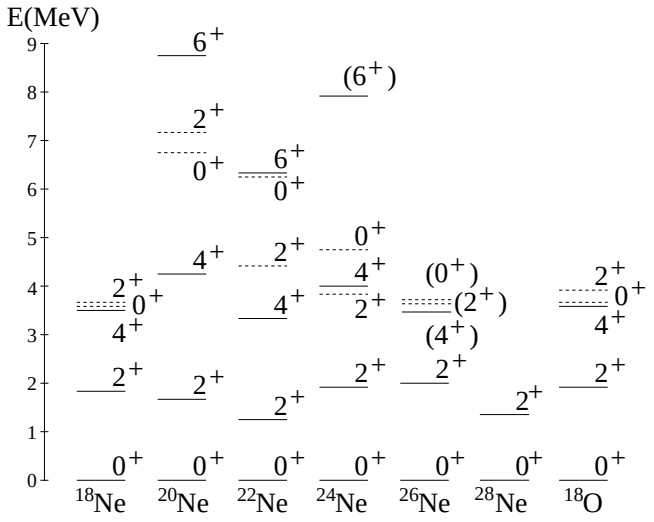

FIG. 12. A comparison of the energies of the lowest 0^+, 2^+, 4^+, and 6^+ and second 0^+ and 2^+ states across the even Ne isotopes.

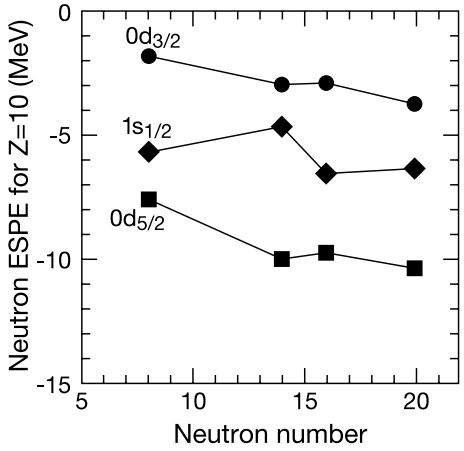

FIG. 13. Variation of the neutron effective single-particle energies implied by the USD interaction for the neon ($Z=10$) isotopes as a function of neutron number.

card into the interpretation of the level scheme. In ^{22}Ne, the lowest intruder state is a 2^- level at 5147 keV. Shell model calculations including the $p_{1/2}$ orbital predict intruder states to appear above 5.4 MeV [12,14]. No good candidate has been identified for this state. The 9.63-MeV state (which is beyond the range studied in the present work) provided the best evidence for negative parity in the (t,p) angular distributions [12]. There was no clear evidence for negative parity below this, although a few angular distributions were not inconsistent with negative parity. Some of the measured γ angular distributions also rule out negative parity, as discussed in the preceding section. Otherwise, an experimental determination of the parities of the states is not possible in the present work because the statistics are far too low to measure the polarizations of the γ transitions using Compton scattering and the energies of the transitions are all much too high to exhibit any measurable internal conversion. One candidate for a 3^- intruder state is the 7248-keV level, although it could also be an s-d state.

C. Systematics

The energies of the lowest 2^+, 4^+, and 6^+ and the second 0^+ and 2^+ states in the even Ne isotopes are compared in Fig. 12. ^{22}Ne exhibits the most rotation-like spectrum of this group and has the lowest 2^+, 4^+, and 6^+ levels. The spacing of these states is also rotationlike in ^{20}Ne, but with what would be called a smaller moment of inertia in a rotational interpretation. Also the second 0^+ and 2^+ states in ^{20,22}Ne do not cluster near the lowest 4^+, as would be expected for a vibrator. By contrast, ^{18}Ne and ^{24}Ne exhibit a more vibration-like spectrum with a 4^+ energy approximately twice that of the lowest 2^+ state and the second 0^+ and 2^+ levels lie close to the first 4^+ one, as would be expected for a two-phonon group. However, the position of the 6^+ state in ^{24}Ne suggests that a more rotation-like behavior may set in at higher spins. ^{26}Ne also appears to exhibit a vibration-like spectrum, although the spin assignments are not firm [15,16], while the low energy of the first (2^+) level in ^{28}Ne [17] suggests a return to higher deformation. The overall pattern is consistent with filling of the $d_{5/2}$ orbital. ^{18}Ne, with a closed $\nu p_{1/2}$ orbital and empty $\nu d_{5/2}$ one, exhibits low collectivity and more spherical properties. Collectivity increases as the $\nu d_{5/2}$ orbital becomes partially filled in ^{20,22}Ne. Then collectivity decreases and more spherical behavior returns when the $\nu d_{5/2}$ orbital is filled at ^{24}Ne. However, neutron excitations out of the $d_{5/2}$ orbital become possible at higher excitation energies and collectivity increases. Thus the sphericity of ^{24}Ne provides information on the shell gap above the $\nu d_{5/2}$ orbital.

The experimentally observed pattern is quite consistent with the shell gaps in the USD interaction. The neutron effective single-particle energies from the USD interaction in the even neon isotopes are graphed as a function of neutron number in Fig. 13. The high energy of the empty $d_{5/2}$ orbital for $N=8$ would lead to lower collectivity in ^{18}Ne. As neutrons begin to fill the $d_{5/2}$ orbital, collectivity depends more on the spacing to the next $s_{1/2}$ orbital, which is moderate for $N=10$ and 12. The spacing reaches a maximum for $N=14$ (^{24}Ne), which again shows lower collectivity. Then the large gap between the filled $s_{1/2}$ orbital and the empty $d_{3/2}$ one also implies low collectivity for $N=16$ (^{26}Ne). The reduced $s_{1/2}$-$d_{3/2}$ gap at $N=18$ is consistent with the lower 2^+ energy in ^{28}Ne, although a greater influence of p-f intruder configurations also contributes to increased collectivity. The only trend not reproduced is the increase in collectivity seen experimentally from $N=10$ to 12, while the increasing single-particle gap would imply the opposite.

The lower level structure of ^{18}O is qualitatively similar to that of ^{24}Ne, with both presenting a vibration-like appearance. This similarity was expected based on the closed neutron $d_{5/2}$ shell in ^{24}Ne. However, the similarities do not extend to higher excitation energies. For example, the lowest 6^+ state in ^{18}O lies at 11.69 MeV, almost 4 MeV higher than in ^{24}Ne. Also counterparts for the cluster of negative-parity states above 4 MeV in ^{18}O have not been observed in ^{24}Ne. In retrospect, the similarities and differences between the

structure of these two nuclei are perhaps to be expected. At low excitation energies both exhibit the spectrum of two $d_{5/2}$ particles—protons for ^{24}Ne and neutrons for ^{18}O. Then at higher energies, excitations of neutrons above the $d_{5/2}$ orbital lead to different positive-parity structure in ^{24}Ne, while excitations of $p_{1/2}$ protons into the empty $d_{5/2}$ orbital lead to lower negative-parity states in ^{18}O.

V. SUMMARY

The combination of a radioactive, but long-lived, ^{14}C target and beam, along with particle-γ and particle-γ-γ coincidences from a modern γ detector array, has provided substantial new insight into the structure of $T=2$ ^{24}Ne. Because of the overwhelming neutron decay back towards stability, electromagnetic transitions in ^{24}Ne were only visible in coincidence with α particles from the ^{14}C(^{14}C,α) reaction. Correlations between α and γ energies and some α-γ-γ coincidences provided the placement of the newly observed transitions in the ^{24}Ne level scheme. Two-point angular distributions led to a number of spin assignments and restrictions.

All but one of the 12 states predicted to lie below 6 MeV by the USD shell model calculations have been observed in the present work. The missing 0_3^+ level was seen in an earlier (t,p) work [12]. The agreement in energy is rather typical for shell model results nearer stability, but there is a systematic tendency for the experimentally observed levels to lie a little higher in energy than the calculated ones. A comparison of predicted and observed decay branches shows good agreement for most of the states, but again significant disagreements for several.

These results are similar to those recently reported from the first study of the level scheme of a $T=\frac{5}{2}$ s-d shell nucleus, ^{27}Na [5]. Together they may suggest the need to restudy the interaction as it applies to nuclei farther from stability. For example, single-particle energies shift with neutron excess, as has been observed in other mass regions [18] as well as in the s-d shell.

Above 6.5 MeV, the lowest 5^+ and 6^+ states have very likely been identified. Their energies and decay patterns agree well with shell model predictions. Beyond these, only about half the predicted number of states has been observed between 6.5 and 8 MeV and correspondences are more tentative.

No negative-parity intruder states have been clearly established although some are generally expected above 5.5 or 6 MeV. Some candidates remain, but negative parity has been ruled out for many of the states observed through nonzero mixing ratios which would imply too strong $M2$ transitions.

A comparison of the structure of the even Ne isotopes suggests a significant shell gap above the $\nu d_{5/2}$ orbital in ^{24}Ne. One sign of this is the spherical, vibration-like structure of ^{24}Ne below 5 MeV, which has a filled $\nu d_{5/2}$ shell. This is rather similar to the structure in ^{18}Ne, which has a closed $p_{1/2}$ shell and empty $\nu d_{5/2}$ orbital, and different from the rotation-like structure of the intervening isotopes ^{20,22}Ne which have a partially filled $\nu d_{5/2}$ orbital. Further evidence comes from similarities with the lower structure of ^{18}O, as described in the preceding section. The neutron effective single-particle energies deduced from the USD interaction do show a large $d_{5/2}$-$s_{1/2}$ gap, as well as other features which correspond to the experimentally observed variation of collectivity across the neon isotopes.

ACKNOWLEDGMENTS

This work was supported in part by the National Science Foundation through Grant Nos. PHY-99-70991 and PHY-01-39950. We are grateful to V. Griffin, E.G. Myers, B.G. Schmidt, J. Janecke, V.G. Goldberg, P. Barber, and Daresbury Laboratory for their contributions to the ^{14}C ion source and targets.

[1] B.A. Brown and B.H. Wildenthal, Annu. Rev. Nucl. Part. Sci. **38**, 29 (1988).
[2] I. Wiedenhöver *et al.*, Phys. Rev. Lett. **87**, 142502 (2001).
[3] D.M. Headly, R.K. Sheline, S.L. Tabor, U.J. Hüttmeier, C.J. Gross, E.F. Moore, B.H. Wildenthal, H.R. Weller, R.M. Whitton, and I. Ragnarsson, Phys. Lett. B **198**, 433 (1987).
[4] D.M. Headly, R.K. Sheline, S.L. Tabor, U.J. Hüttmeier, C.J. Gross, E.F. Moore, B.H. Wildenthal, H.R. Weller, R.M. Whitton, and I. Ragnarsson, Phys. Rev. C **38**, 1698 (1988).
[5] M.W. Cooper, S.L. Tabor, T. Baldwin, D.B. Campbell, C. Chandler, C.R. Hoffman, K.W. Kemper, J. Pavan, A. Pipidis, M.A. Riley, and M. Wiedeking, Phys. Rev. C **65**, 051302(R) (2002).
[6] R.G.H. Robertson and B.H. Wildenthal, Phys. Rev. C **8**, 241 (1973).
[7] M.G. Silbert and N. Jarmie, Phys. Rev. **123**, 221 (1961).
[8] J.A. Becker, L.F. Chase, Jr., R.E. McDonald, and E.K. Warburton, Phys. Rev. **176**, 1310 (1968).
[9] A.J. Howard, R.G. Hirko, and D.A. Bromley, Phys. Rev. C **1**, 1446 (1970).
[10] B.A. Watson, J.A. Becker, and T.R. Fisher, Phys. Rev. C **9**, 1200 (1974).
[11] K. Bharuth-Ram, K.P. Jackson, K.W. Jones, and E.K. Warburton, Nucl. Phys. **A137**, 262 (1969).
[12] N.M. Clarke, M.B. Becha, P.R. Hayes, and K.I. Pearce, J. Phys. G **15**, 863 (1989).
[13] R. Maier, G. Korschinek, P. Spolaore, W. Kutschera, H.J. Maier, and W. Goldstein, Nucl. Instrum. Methods **155**, 55 (1978).
[14] J.B. McGrory and B.H. Wildenthal, Phys. Rev. C **7**, 974 (1973).
[15] A.T. Reed *et al.*, Phys. Rev. C **60**, 024311 (1999).
[16] O. Sorlin, Nucl. Phys. **A685**, 186c (2001).
[17] B.V. Pritychenko *et al.*, Phys. Lett. B **461**, 322 (1999).
[18] Gillis Carlsson, Masters thesis, University of Lund, 2003.